

Photocatalytic degradation of flexible PVC/TiO₂ nanohybrid as an eco-friendly alternative to the current waste landfill and dioxin-emitting incineration of post-use PVC

Sung Ho Kim^a, Seung-Yeop Kwak^{a,*}, Takenori Suzuki^b

^a *Hyperstructured Organic Materials Research Center (HOMRC) and School of Materials Science and Engineering, Seoul National University, San 56-1, Shillim-dong, Gwanak-gu, Seoul 151-744, South Korea*

^b *Radiation Science Center, High Energy Accelerator Research Organization (KEK), Tsukuba, Ibaraki 305-0801, Japan*

Received 20 November 2005; received in revised form 27 February 2006; accepted 6 March 2006

Abstract

Photo-degradable poly(vinyl chloride) (PVC)/titanium dioxide (TiO₂) nanohybrid has been investigated to be utilized as an eco-friendly alternative strategy to the current waste landfill and toxic byproduct-emitting incineration of PVC wastes. Thus, the present study suggests a novel idea related to preparing the photocatalytically degradable nanohybrid through TiO₂ nanoparticle-integrated hyperbranched poly(ϵ -caprolactone) (HPCL–TiO₂). The main aim of this study is to find a solution to the unresolved problem in the conventional PVC/TiO₂ composites related to the poor dispersion of the nanoparticles in PVC polymer. First, TiO₂ nanoparticles are prepared by a sol–gel process, and the size of the particle is about 5–10 nm in diameter as measured by using a transmission electron microscopy (TEM) and dynamic light scattering (DLS). The hyperbranched poly(ϵ -caprolactone) (HPCL) with numerous COOH groups and good miscibility with PVC as a binder for TiO₂ nanoparticles is prepared from moisture-sensitive catalyst-free polymerization of 2,2-bis[ω -hydroxy oligo(ϵ -caprolactone)methyl]propionic acids followed by modification reaction using pyridinium dichloromate (PDC), then characterized with ¹H NMR and ¹³C NMR analyses. The integration of TiO₂ nanoparticles onto HPCL is carried out by a dip-coating method based on the spontaneous self-assembly between TiO₂ nanoparticles and HPCL, and the loading amount of the nanoparticles in the HPCL–TiO₂ is determined to be ca. 3.3 wt% by X-ray photoelectron spectroscopy (XPS). Then, the HPCL–TiO₂ is blended with PVC by solution blending in THF as solvent, and the resulting dispersibility of TiO₂ nanoparticle in PVC is characterized by field emission scanning electron microscopy (FESEM) equipped with energy dispersive spectrometry (EDS), which exhibits the TiO₂ nanoparticles are well-dispersed in PVC matrix, while some agglomerates are observed in the PVC/TiO₂ sample prepared from TiO₂ nanoparticle itself. The photocatalytic degradation of the samples are examined and verified from the change of surface morphology, chemical structure, molecular weight, and molecular-level structure after UV irradiation through field-emission scanning electron microscopy (FESEM), UV–visible spectroscopy, gel permeation chromatography (GPC), and positron annihilation lifetime spectroscopy (PALS). The remarkable photocatalytic degradation is observed in the PVC/HPCL–TiO₂, and the structural change accompanied by the degradation of the irradiated sample can clearly explained.

© 2006 Elsevier Ltd. All rights reserved.

Keywords: Poly(vinyl chloride) (PVC); Titanium dioxide (TiO₂); Photocatalytic degradation

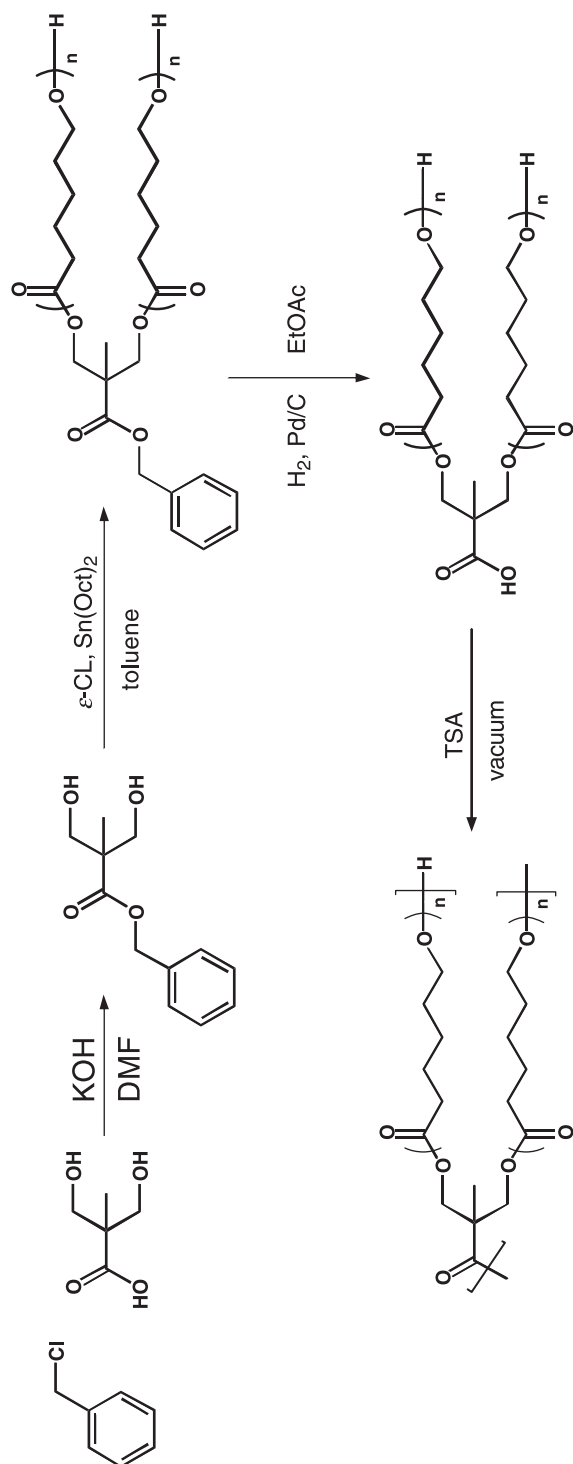
1. Introduction

Poly(vinyl chloride) (PVC) is one of the most widely used polymers in the world, because it exhibits a good price/performance balance that allows penetration into many applications such as pipes, cable insulation, packaging foils,

and medical products [1]. When the lifetime of all these articles expires, we are left with a large bulk of scrap waste, which in turn raises public concern about how these wastes should be disposed. Although the waste treatment through incineration process has many advantages of a high degree of destruction, the reduced land usage, and the potential for energy recovery, the incineration of PVC can cause serious environmental problems such as toxic dioxin emission from inadequate equipment or inappropriate incineration. Therefore, in this study, we attempted to investigate the photocatalytic degradation of wasted PVC as an eco-friendly alternative of disposal method [2–4].

* Corresponding author. Tel.: +82 2 880 8365, fax: +82 2 885 1748.

E-mail address: sykwak@snu.ac.kr (S.-Y. Kwak).

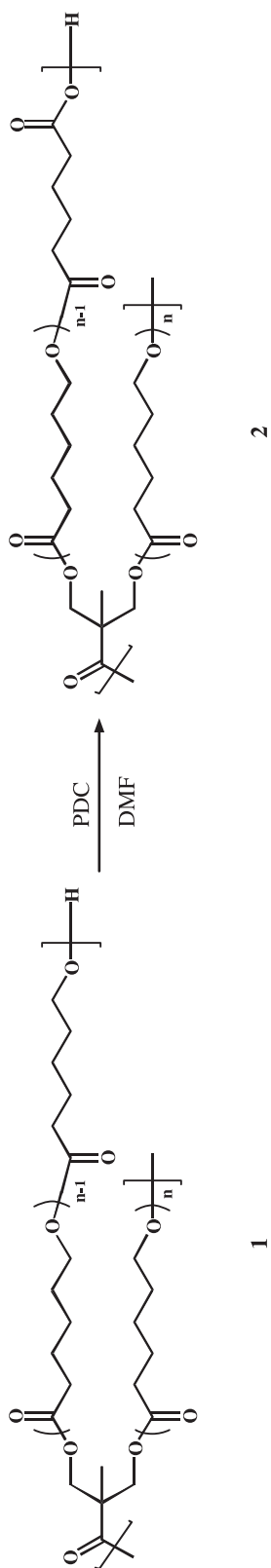


Scheme 1.

Titanium dioxide (TiO₂) nanoparticles have been investigated in recent years, particularly because of their photocatalytic effects that decompose various organic chemicals and polymers such as polyethylene (PE), polystyrene (PS), PVC and so on [5,6]. Especially, several studies on photocatalytic and/or photolytic degradation of TiO₂-blended PVC have been carried out [3,4]. The TiO₂ photocatalysis is known to generate active oxygen species, e.g. O₂⁻, HO₂[·], HO[·], from H₂O or O₂ by oxidative or reductive reactions under UV [4]. These active oxygen species lead to the degradation reaction by attacking polymer chain and successive chain cleavage. Although the previous study demonstrated that the polymer–TiO₂ composite showed a potential viability to be used as a photodegradable product, there still remain some unresolved matters related to the uniform dispersion of photocatalyst in polymer matrix. The micrometer-sized agglomerates of TiO₂ nanoparticles can significantly reduce the efficiency of photodegradation through the decrease of the interfacial areas between PVC and TiO₂. Thus, in order to promote the dispersion of TiO₂ nanoparticles in PVC, we tried to prepare nano-sized TiO₂ particle-integrated hybrid polymer to be blended with PVC.

Hyperbranched polymers (HBPs) are highly branched macromolecules with highly functionalized globular architectures, which have attracted much attention as materials with unique properties and new application potentials in comparison to the linear polymer [7,8]. Poly(ϵ -caprolactone) (PCL) is one of the widely used biodegradable polymers, and it is reported to have good miscibility with varieties of polymer including PVC [9]. In our previous study, we prepared hyperbranched poly(ϵ -caprolactone) (HPCL) with dendritic globular structure, which allows the HPCL to exhibit different properties as those of its linear counterpart with the same molecular weight, such as less entanglement in the solid state, low melt viscosity, and fast molecular motion [10,11]. The HPCL with numerous functional ends due to unique dendritic architecture shows a good potential to be used as a substitute for PVC plasticizer. Therefore, the use of HPCL as a binder for TiO₂ incorporation could endow the final PVC/TiO₂ product with remarkable flexibility as well as numerous functional ends.

There are various strategies for incorporating TiO₂ nanoparticles on the target materials, e.g. sol–gel synthesis, sputtering, chemical vapor deposition (CVD), and so on [12]. Among them, the self-assembly method which is based on the spontaneous adsorption property between polymer and TiO₂ particles is expected to be a strong candidate, overcoming the limitations inherently associated with other methods, i.e. high temperature, costly fabrication, and complex process control [13–15]. The mechanism of self-assembly behavior of TiO₂ on polymer with COOH groups was previously investigated by virtue of diffuse reflectance infrared Fourier transform (DRIFT) [16], which showed that TiO₂ becomes adsorbed and bound on polymer with a considerable strength as a result of the formation of the bidentate coordination and H-bond between TiO₂ and polymer. It is possible to apply the self-assembly method to preparation of TiO₂-incorporated HPCL (HPCL–TiO₂) by modifying HPCL to have carboxylic acid functional groups.



Scheme 2.

In this study, the pyridinium dichromate (PDC) oxidation reaction is utilized to modify the HPCL which was prepared through moisture-sensitive catalyst-free polymerization of 2,2-bis[ω -hydroxy oligo(ϵ -caprolactone)methyl]propionic acids. TiO_2 nanoparticles could be incorporated with the modified HPCL through the self-assembly process and form a HPCL– TiO_2 without forming agglomerates. The novel HPCL– TiO_2 makes it possible to prepare photodegradable PVC/ TiO_2 nanohybrid, aiming at a breakthrough of the unresolved problem of conventional PVC/ TiO_2 composites related with the poor dispersion of the nanoparticles in the PVC matrix. The degree of dispersion of TiO_2 in the PVC/HPCL– TiO_2 nanohybrid is observed and compared with that of the PVC/ TiO_2 composite prepared from solution-blending of PVC with a similar content of TiO_2 . Investigation on the degradation behavior of PVC/HPCL– TiO_2 under UV irradiation through various characterization methods could give an efficient evidence for successful introduction of TiO_2 into PVC and actual validity of this approach.

2. Experimental section

2.1. Preparation of TiO_2 nanoparticles

TiO_2 nanoparticles were prepared from the controlled hydrolysis of titanium tetraisopropoxide, $\text{Ti}(\text{OCH}(\text{CH}_3)_2)_4$, in accordance with the procedures as described in the literature [17]. A 1.25 mL of $\text{Ti}(\text{OCH}(\text{CH}_3)_2)_4$ (Aldrich, 97%) dissolved in 25 mL of absolute ethanol was added drop by drop under vigorous stirring to 250 mL of distilled water (4 °C) adjusted to pH 1.5 with nitric acid. This mixture was stirred overnight until it was clear and the transparent colloidal suspension (1.34 g/L) resulted. To obtain powder sample, the colloidal suspension was evaporated at 35 °C using a rotavapor and dried under vacuum oven. The size of powdered TiO_2 particle was determined by a JEOL JEM-200CX transmission electron microscope (TEM) at 120 kV. For the TEM observation, the TiO_2 colloidal suspension was dropped on a carbon-coated grid and then dried at room temperature. Redissolving the TiO_2 powder in distilled water with 0.5 g of TiO_2/L resulted in a transparent suspension of $\text{pH } 2.8 \pm 0.1$. The hydrodynamic colloidal particle size was measured by dynamic light scattering method using a photon correlation spectroscopy system (DLS-7000, Otsuka Electric) utilizing an Ar laser at a scattering angle of 90°.

2.2. Preparation of hyperbranched poly(ϵ -caprolactone) (HPCL) with carboxylic acid groups

Hyperbranched poly(ϵ -caprolactone) (HPCL) with numerous COOH groups was prepared as following the procedure as shown in Schemes 1 and 2. First, hyperbranched poly(ϵ -caprolactone) was prepared by moisture-sensitive catalyst-free polymerization of AB_2 macromonomer, 2,2-bis[ω -hydroxy oligo(ϵ -caprolactone)methyl]propionic acids. Details on the synthesis and characterization of the materials in Scheme 1 had already been described in our previous reports [10,11]. Then,



Fig. 1. TEM micrograph of the TiO₂ nanoparticles.

the hyperbranched poly(ϵ -caprolactone) (HPCL), **1**, was modified to **2** with acid derivatives by oxidation reaction in dimethylformamide (DMF) using pyridinium dichromate (PDC) as reagent (Scheme 2) [18]. Six grams of polymer **1** and 6 g of PDC was dissolved in DMF, and the reaction was carried out at 25 °C for 24 h. At the end of the reaction, the mixture was precipitated into an excess of distilled water, washed thoroughly several times and filtered out to give **2** as white solids. Yield: ca. 90%. The modification of HPCL was confirmed by ¹H NMR and ¹³C NMR, employing a Bruker Avance DPX-300 spectrometer with the tetramethylsilane (TMS) signal as an internal standard in CDCl₃.

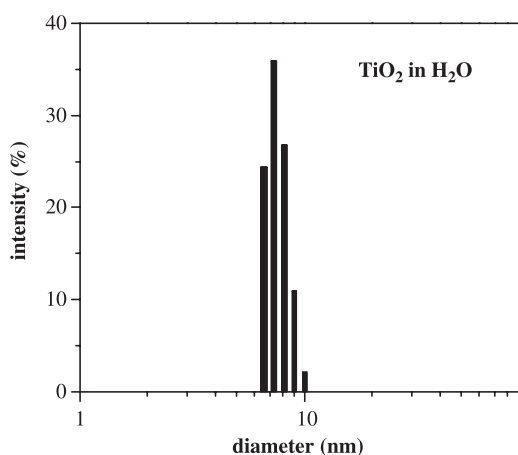


Fig. 2. Size distribution of the TiO₂ nanoparticles in water.

Table 1
General characteristics of hyperbranched poly(ϵ -caprolactone)

Sample	[ϵ -CL] ₀ /[–OH] ^a	<i>n</i> ^b	$\langle N_{AB_2} \rangle^c$	M_n^d	M_w/M_n^d
HPCL (1)	10	10.3	5.1	12,600	1.6

^a Ratio of ϵ -caprolactone monomer to initiating hydroxyl group.

^b Average number of ϵ -caprolactone units in AB₂ macromonomers determined by ¹H NMR measurement.

^c Number of the AB₂ macromonomer in HPCLs determined from ¹H NMR.

^d Molecular weight and distribution obtained from SEC-MALLS.

2.3. Introduction of TiO₂ nanoparticle onto HPCL polymers (HPCL–TiO₂)

The incorporation of TiO₂ particles with HPCL was carried out by dip-coating method based on spontaneous self-assembly property between TiO₂ and polymer with COOH groups [13]. Two grams of **2** was dipped in 1 L of the transparent TiO₂ colloidal solution (0.5 g TiO₂/1 L H₂O) for 3 h to deposit TiO₂ nanoparticles on **2**. An excess of TiO₂ solution was filtered off and removed to give HPCL–TiO₂, which was thoroughly washed with distilled water and dried under vacuum. The HPCL–TiO₂ was characterized by X-ray photoelectron spectroscopy (XPS) employing a Kratos AXIS HS spectrometer with Mg K α X-ray source (1253.6 eV). The X-ray gun was operated at 10 kV and 1 mA, and the charge neutralization system was used to obtain high resolution spectra for the insulating materials such as polymers by reducing the surface charge. The elemental composition analysis was performed on carbon, oxygen, and titanium. The sensitivity factors for individual elements were taken with the values from the library provided by the manufacturer.

2.4. Blending of PVC with HPCL–TiO₂ and investigation of dispersibility of TiO₂ in the blend

Poly(vinyl chloride) (PVC) for the blend was P-800 (Hanwha Chem Co.) with M_n of about 50,000. The blend of PVC with HPCL–TiO₂ was prepared by solution blending with tetrahydrofuran (THF) as solvent. Three grams of PVC and 2 g of HPCL–TiO₂ were dissolved in 200 mL of THF, and the mixture was stirred vigorously to obtain homogeneity. Then, the solvent was evaporated at 40 °C for 24 h, then the PVC film was further dried in a vacuum oven until no further weight loss was observed. The thickness of the resulting PVC/HPCL–TiO₂ (60/40) film was measured to be ca. 0.2 mm. The dispersibility and contents of TiO₂ nanoparticles in PVC/HPCL–TiO₂ films were investigated by a JEOL JSM-6700F field emission scanning electron microscope (FESEM) equipped with an energy dispersive spectrometer (EDS) employing an exciting electron beam of 20 keV. Inca 2000 program was used to deconvolve the energy-dispersive spectra and make quantitative analyses. The result on the contents of constituent atoms in the film was determined by multiple replications. For comparison, FESEM/EDS analyses were also performed on PVC/TiO₂ sample which was prepared from solution blending of TiO₂ nanoparticle with PVC dissolved in THF.

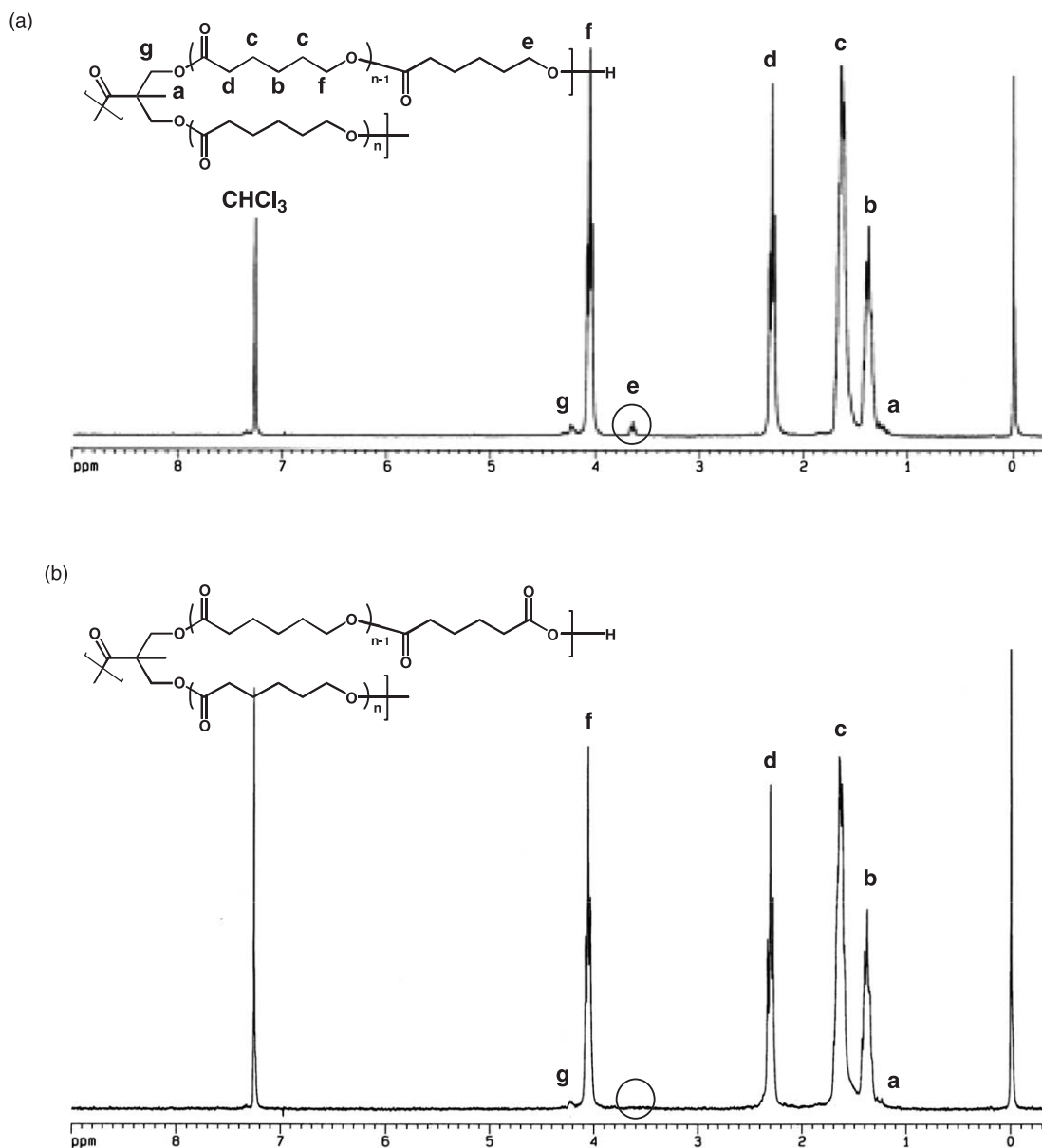


Fig. 3. ¹H NMR spectra of HPCLs before, (a), and after, (b), modification reaction.

2.5. Photocatalytic degradation of PVC/HPCL–TiO₂ film

The PVC/HPCL–TiO₂ film was placed in 100 mL of deionized water contained in a glass beaker. The intensity of solar light was reported be ~ 4.1 mW/cm² at 260 nm and ~ 5.3 mW/cm² at 360 nm [2]. The artificial medium-wave UV lamp (XX-15B, Spectroline) equipped with two 15 W tubes and long life filter assembly was used in this experiment. The light intensity at the typical peak of 312 nm was ca. 1100 μ W/cm² at 25 cm, which was provided by the manufacturer. After illumination up to the intended exposure time, the films were dried and surface morphological images of the exposed films were taken by using a Jeol JSM-6630F FESEM with the pre-treatment of Pt deposition. For comparison, PVC/HPCL films without TiO₂ nanoparticles were also prepared and investigated before and after irradiation.

The UV–visible spectrum was recorded with a Hewlett–Packard HP8452 diode array spectrophotometer to analyze the optical absorption characteristics of the irradiated samples and to characterize the chemical structural changes accompanied by photocatalytic degradation. The distribution of molecular weights in the PVC/HPCL–TiO₂ after appropriate irradiation periods was determined by gel permeation chromatograph equipped with Shodex GPC columns and a Sung Jin I&T liquid chromatograph. Tetrahydrofuran was used as the eluent.

Further study on the effects of the photocatalytic degradation on the molecular-level structure was characterized by using positron annihilation lifetime spectroscopy (PALS). The PALS experiments were performed by using a conventional fast–fast coincidence system at room temperature. A positron source was sandwiched between the films that were stacked to

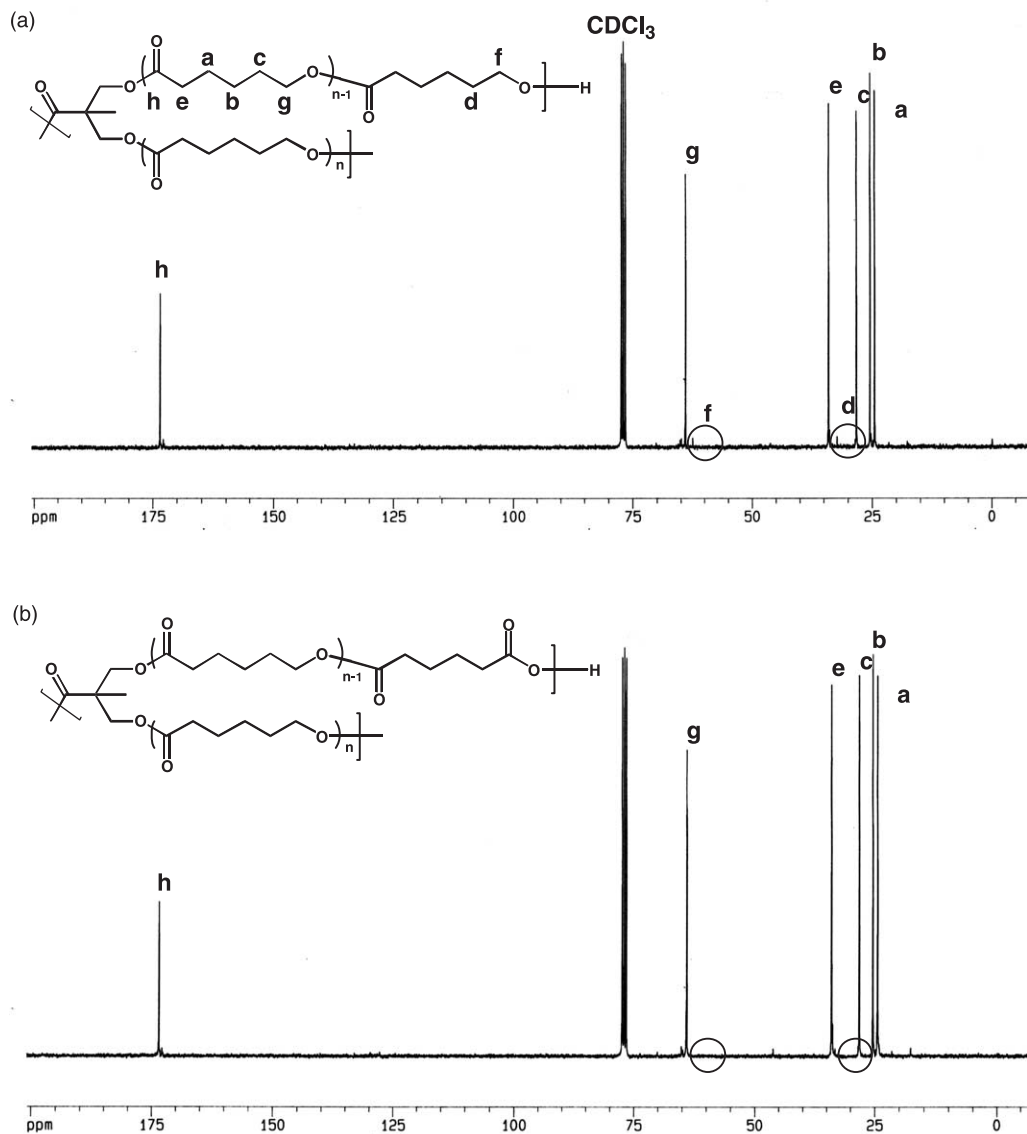


Fig. 4. ^{13}C NMR spectra of HPCLs before, (a), and after, (b), PDC modification.

a thickness of approximately 1 mm. The γ -rays with energies of 1.27 MeV (emitted from a β -decay of ^{22}Na source) and those of 0.511 MeV (emitted from a positron annihilation in a sample) were measured by the start and the stop counters, respectively. Each spectrum has counts of about four millions and a time resolution of about 300 ps full-width at half maximum (FWHM). The average lifetime and the lifetime distribution of spectra were analyzed through two methods: a finite-term lifetime analysis and a continuous lifetime analysis using PATFIT and MELT programs, respectively [19,20].

3. Results and discussion

3.1. Particle size of TiO_2 nanoparticles

The TEM image of the prepared TiO_2 particles is shown in Fig. 1, where black spots are the TiO_2 nanoparticles

prepared via sol-gel synthesis of titanium isopropoxide. The mean diameter of the TiO_2 powder is less than 10 nm. Dynamic light scattering (DLS) was also used to determine the particle size of TiO_2 nanoparticles re-dissolved in deionized water. Particles in small size show moment-by-moment shift of their positions, orientations and shapes owing to Brownian motions such as translation, rotation, etc. in a solution. This method is based on the intensity of scattered laser light, which is measured by periods and depends on the particle size. As small particles are influenced more by Brownian molecular motion of the water molecules in the dispersion medium, they diffuse faster than the larger ones. The DLS measurement of TiO_2 solution in Fig. 2 shows the particle sizes and particle size distribution of TiO_2 nanoparticles in water. The particle size is 7.6 ± 0.7 nm in diameter, which is in good agreement with TEM observations.

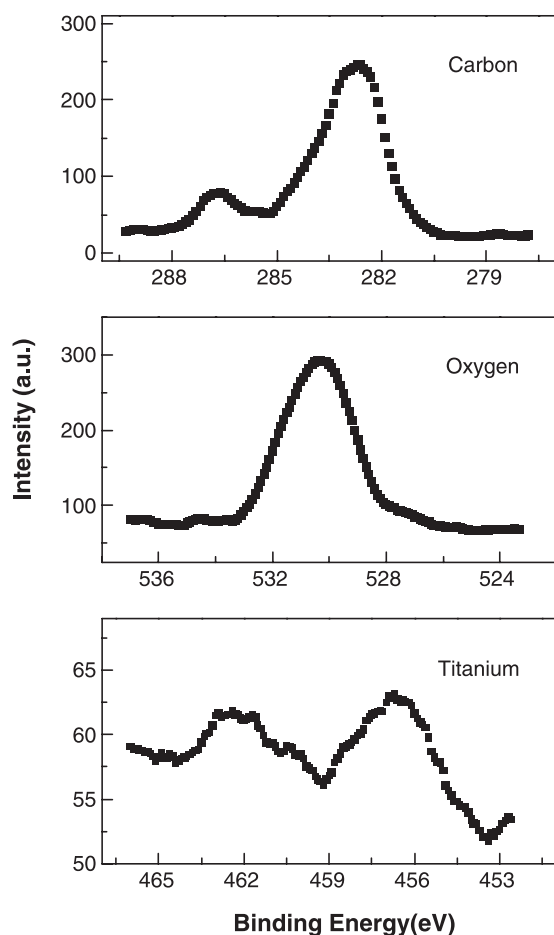


Fig. 5. XPS spectra of carbon, oxygen, and titanium for HPCL–TiO₂ sample.

3.2. Hyperbranched poly(ϵ -caprolactone) (HPCL) with carboxylic acid groups

The synthesis of the HPCL with numerous hydroxyl terminal groups, **1**, was performed according to the procedure in our previous works (Scheme 1), and the general characteristics of **1** are listed in Table 1 [10,11]. The values of $[\epsilon\text{-CL}]_0/[\text{-OH}]$ and n are the targeted and calculated number of ϵ -caprolactone monomer units incorporated in the AB₂ macromonomer, respectively. The average number of the AB₂ macromonomer units incorporated in the HPCL polymer,

$\langle N_{\text{AB}_2} \rangle$, and the number of the functional end groups, $\langle N_{\text{AB}_2} \rangle + 1$, are easily determined from the relative peak areas of ¹H NMR spectrum and the branching theories developed by Flory, as follows [21]:

$$A_e : A_d = \langle N_{\text{AB}_2} \rangle + 1 : 2n\langle N_{\text{AB}_2} \rangle$$

$$\langle N_{\text{AB}_2} \rangle = \frac{A_d}{2n(A_e - A_d)} \quad (1)$$

where A_e and A_d represent the integrated areas of peak e and d of **1**, respectively, as shown in Fig. 3(a).

The method of self-assembly of TiO₂ on the surface with the terminal functional groups, e.g. –SO₃H or –COOH groups, has been used as a promising technique to immobilize catalytic nanoparticles with maintaining the nanostructure [13–15]. For easier adsorption of TiO₂ onto HPCL, hydroxyl groups of **1** are oxidized to carboxylic acids by using PDC in DMF. ¹H NMR spectra before and after the PDC reaction show that the proton peak assigned to the chain ends (–CH₂–OH, 3.59 ppm) has disappeared, and the value of d - f increases with the oxidation reaction, which indicate the conversion of –CH₂OH to –COOH (Fig. 3). Fig. 4 shows ¹³C NMR spectra of HPCLs. From this figure, we can clearly see that the terminal carbon peaks of f (–CH₂–OH, 61.5 ppm) and d (–CH₂–CH₂OH, 32.2 ppm) are shifted and disappeared during the modification reaction. The combined data of ¹H NMR and ¹³C NMR suggest that the modification of HPCL was successfully performed without any byproduct formed.

3.3. Preparation of TiO₂-integrated HPCL (HPCL–TiO₂)

As described earlier, the HPCL–TiO₂ was prepared by dipping the modified HPCL, **2**, into a solution of TiO₂ nanoparticles, after which it was washed with water. Then, the HPCL–TiO₂ was characterized by X-ray photoelectron spectroscopy (XPS). The XPS analysis is performed on the constituent elements of carbon, oxygen and titanium, as shown in Fig. 5. All the photoelectron peaks appear at positions similar to the reported values of core-electron binding energy, and the presence of Ti peak in XPS spectra of the sample provides the evidence of self-assembly of TiO₂ onto HPCL. From the observed XPS peaks, the relative atomic concentration of the individual elements can be calculated as follows:

$$C_i = \frac{A_i/S_i}{\sum_j^m A_j/S_j} \quad (2)$$

where A_i is the photoelectron peak area of the element i , S_i is the sensitivity factor for the element i , and m ($=3$) is the number of measuring elements. The atomic compositions of C, O, Ti atoms in HPCL–TiO₂ are represented in Table 2. The content of TiO₂ was approximately calculated from the theoretical atomic ratio of chemical formula of TiO₂ and HPCL, yielding an amount of about 3.3 wt% TiO₂ in HPCL–TiO₂.

Table 2
Elemental composition of HPCL–TiO₂ and PVC/HPCL–TiO₂ blends

TiO ₂	HPCL (2)	HPCL–TiO ₂		
Ti/O ^a	C/O/H ^a	C/O/Ti ^b	HPCL ^c	TiO ₂ ^c
1/2	625/222/1030	72.5/26.9/0.6	96.7	3.3
PVC/HPCL–TiO ₂ Blend				
C/O/Cl/Ti ^b	PVC ^c	HPCL ^c	TiO ₂ ^c	
71.38/11.04/17.32/0.26	61.03	37.80	1.18	

^a Theoretical atomic ratios of chemical formulas of TiO₂ or HPCL.

^b Atomic concentrations of elements obtained from XPS or FESEM/EDS analyses.

^c Weight fractions of constituents in HPCL–TiO₂ or PVC/HPCL–TiO₂ blend.

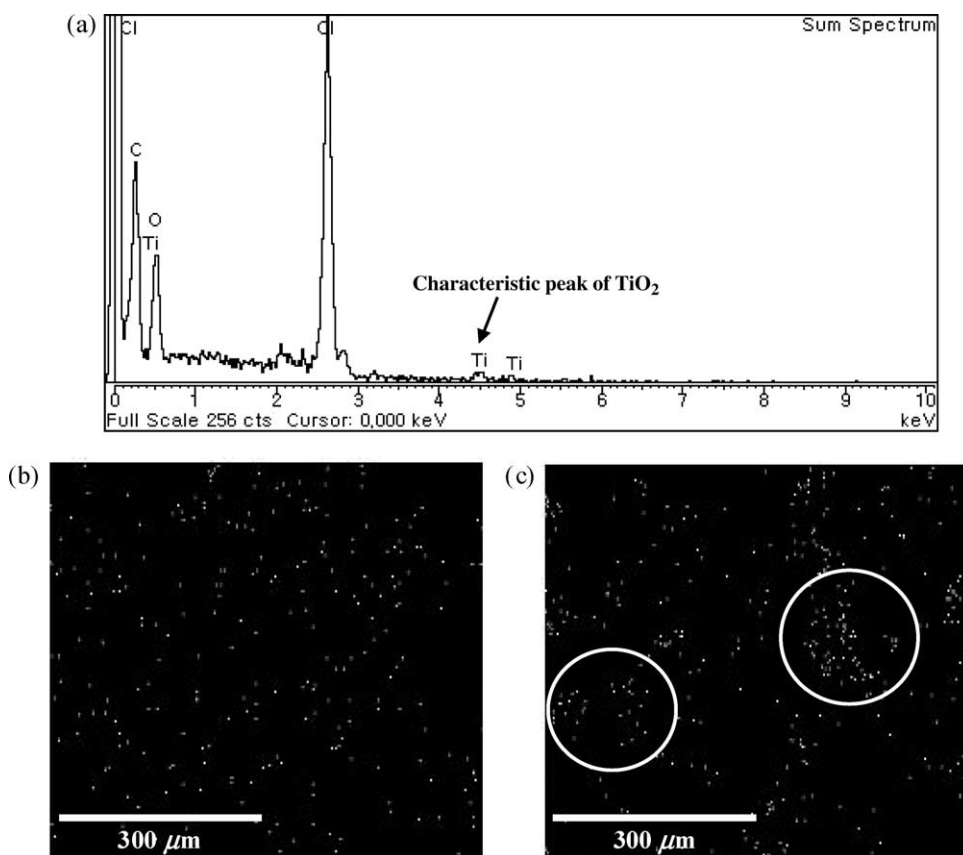


Fig. 6. Energy-dispersive X-ray spectrum, (a), and FESEM/EDS images of PVC/HPCL–TiO₂, (b), and PVC/TiO₂, (c), composed of a similar content of TiO₂.

3.4. Blending of PVC with HPCL–TiO₂ and characterization of dispersibility of TiO₂ in the blend

In order to enhance the dispersibility of TiO₂ in PVC matrix, PVC was blended with not the TiO₂ itself but HPCL–TiO₂ through a solution blending process in THF as solvent. Poor dispersion due to agglomeration of TiO₂ nanoparticles has been known to be one of the main causes to deteriorate the photocatalytic degradation efficiency. The degree of dispersion of TiO₂ in PVC/HPCL–TiO₂ films is characterized by Ti mapping images which employ K α peak of Ti with FESEM/EDS. Fig. 6 shows FESEM/EDS surface images of PVC/HPCL–TiO₂ in conjunction with PVC/TiO₂ sample prepared from solution blending of PVC with TiO₂ itself. The PVC/HPCL–TiO₂ exhibits a good dispersion of TiO₂ in PVC matrix, while some agglomerates of TiO₂ are observed in PVC/TiO₂ with containing a similar content of TiO₂ (Fig. 6(c)). The uniform dispersion of TiO₂ nanoparticles in the polymer matrix is expected to enhance the photocatalytic activity of photodegradable materials for further applications.

3.5. Photocatalytic degradation of PVC/HPCL–TiO₂ Film

FESEM analyses were carried out to examine the surface morphology of the irradiated PVC/HPCL–TiO₂ films. Fig. 7(a) through (d) show the surface images of the PVC/HPCL–TiO₂ films that were irradiated for 0, 10, 20, and 30 days, respectively. The agglomerate of TiO₂ nanoparticles can not

be seen in PVC/HPCL–TiO₂ samples before the irradiation due to the good dispersion of TiO₂ in PVC matrix. The FESEM images reveal that the photocatalytic degradation of PVC leads to the formation of cavities in a sub-micrometer or a few micron size, which is slightly smaller than that reported in previous researches. Considering that the degradation of the PVC matrix is initiated from the interface between PVC and TiO₂ particles [4], the formation of such small cavities is thought to be due to a good dispersion of the nano-sized TiO₂ particles in PVC without forming agglomerates in a large size. The number of holes in PVC/HPCL–TiO₂ increases with irradiation time, and the individual holes get interconnected, while no large hole is observed in the neat PVC/HPCL without TiO₂ nanoparticles after UV exposure for the same period, as shown in Fig. 7(e) and (f). These facts demonstrate that the PVC/HPCL–TiO₂ can be efficiently decomposed by photocatalytic reaction of the incorporated TiO₂ particles, which can be the main evidence for successful incorporation of TiO₂ into PVC matrix and actual validity of this approach.

Fig. 8 shows the UV–visible absorption spectrum of PVC/HPCL–TiO₂ films with and without UV illumination as a function of day. The absorbance at the wavelength in range of 350–550 nm is enhanced with increasing the irradiation time. Based on the foregoing fact that TiO₂ photocatalysis generates active oxygen species such as hydroxyl radicals, and PVC radical can be formed from the attack of the active oxygens, these changes of absorbance could be explained by virtue of the double bonds and their conjugation formed through the intramolecular

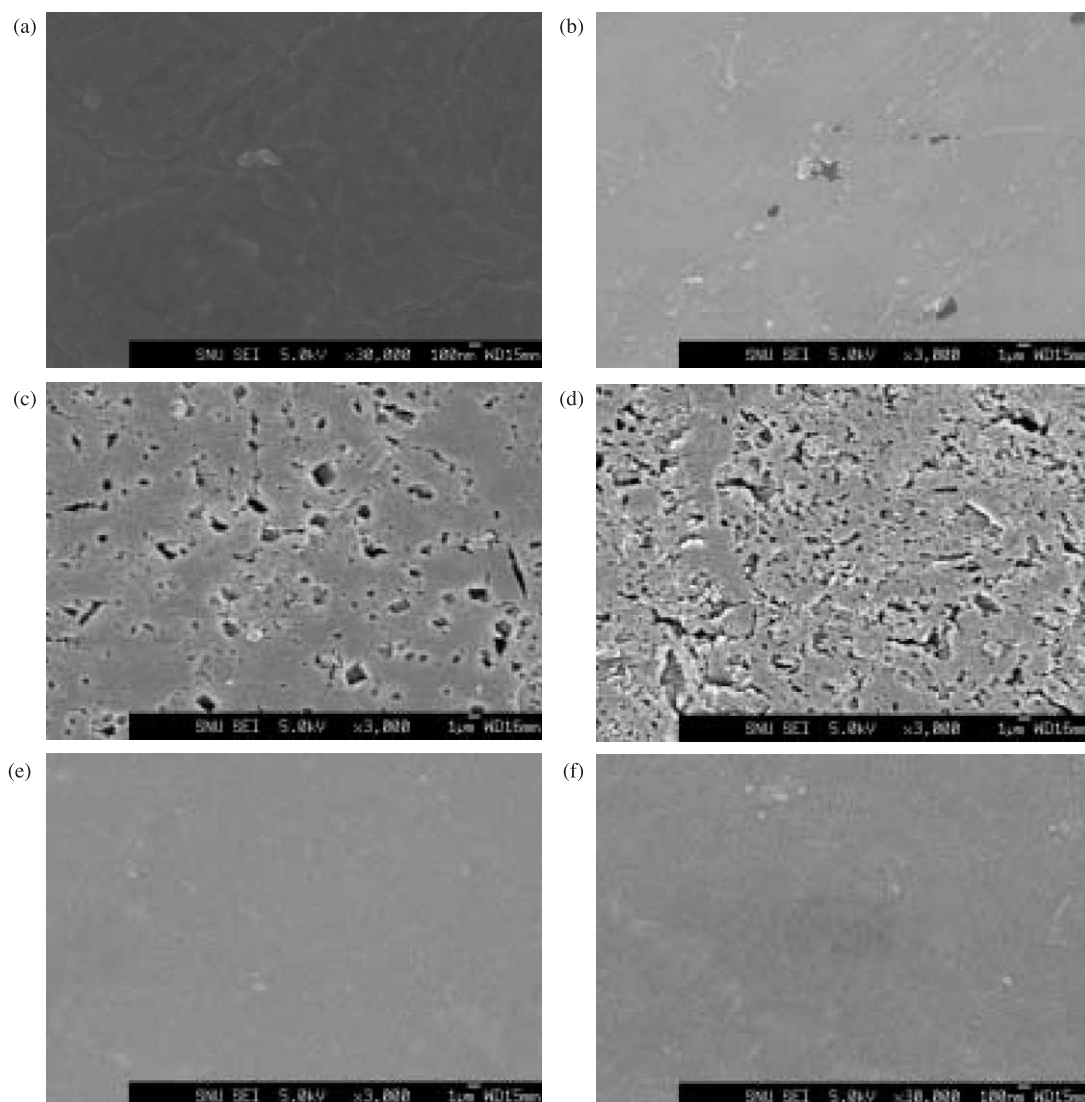


Fig. 7. FESEM micrographs of PVC/HPCL-TiO₂ after 0 day (a), 10 days (b), 20 days (c), and 30 days (d), UV illumination and those of PVC/HPCL after 0 day (e), and 30 days (f), UV exposure.

recombination of the PVC radical. The absorption at the wavelength in this range is assigned to be due to the conjugated double bonds in the literatures [4,22,23]. Fig. 9 depicts gel permeation chromatograms of PVC/HPCL-TiO₂ films at various

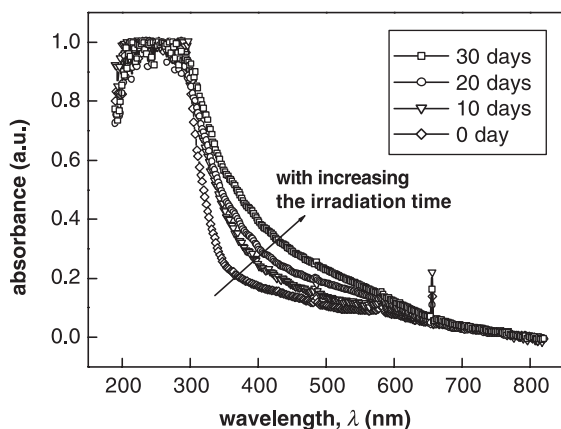


Fig. 8. UV-visible absorption spectra of the irradiated PVC/HPCL-TiO₂.

exposure times. The smooth and mono-modal chromatogram is observed for the non-irradiated sample. On irradiation, the PVC peak becomes a bimodal distribution, in which the right side of the peak indicates cleavage of the PVC chains and formation of fragments with lower molecular weights. Additionally, several peaks also appear in the left side of the main peak, which might be attributed to the byproducts of a large molecular weight formed through the intermolecular recombination of PVC radicals, as was reported in the literature [24].

The degradation of PVC through TiO₂ photocatalysis is initiated from the attack of active oxygen species onto PVC molecules and progressed with the scission and/or recombination of the formed PVC radical molecules. Regardless of the importance in the investigation of the structural change in the atomic- and molecular-level, it is seldom performed due to the difficulty in the measurement on a very small scale. Thus, the continuing study on a molecular-level structural change could also play an important role in understanding the macroscopic degradation behavior of PVC/TiO₂ nanohybrid.

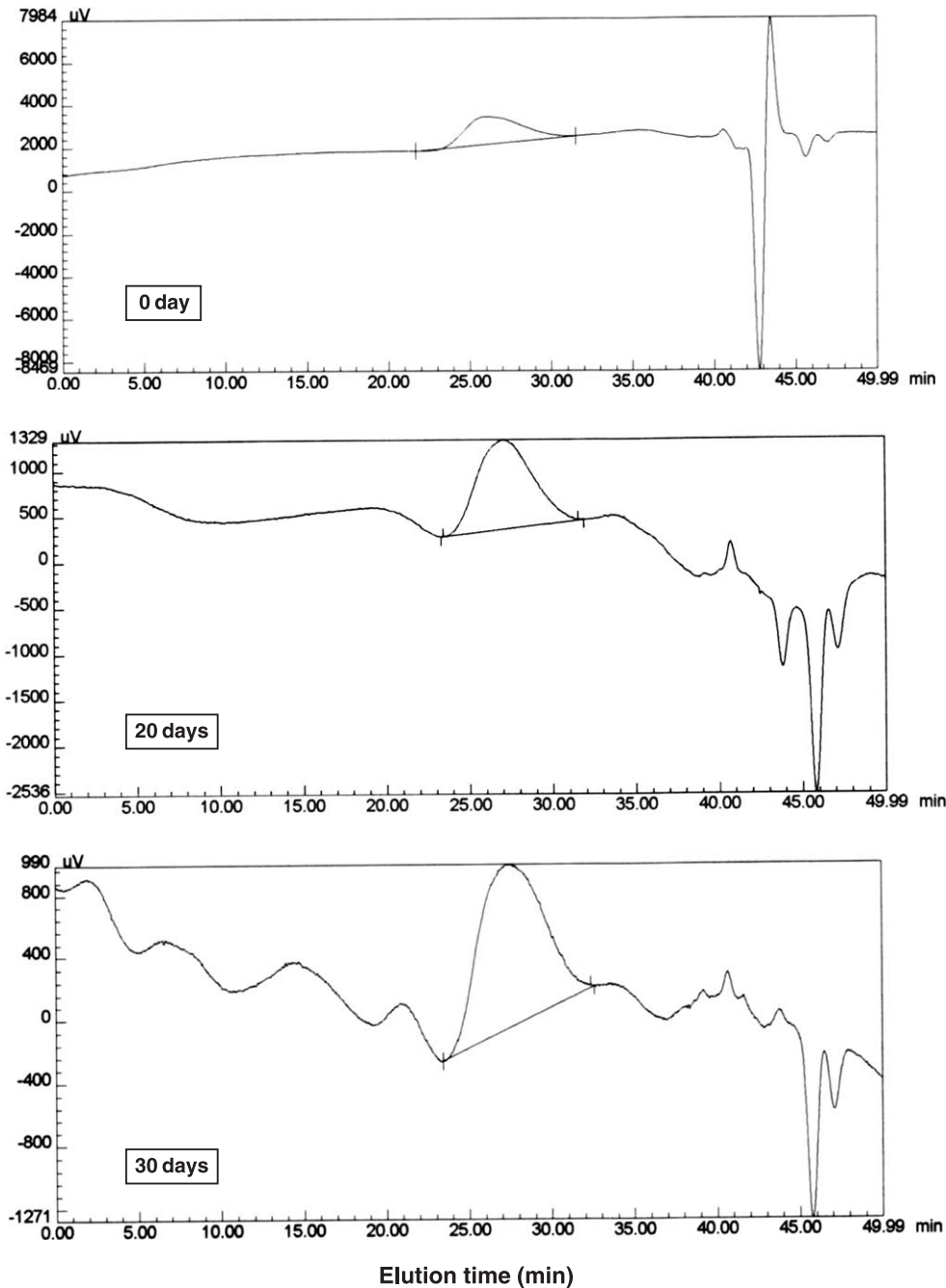


Fig. 9. Gel permeation chromatograms of PVC/HPCL-TiO₂ films at various exposure times.

3.6. Positron annihilation lifetime spectroscopy (PALS)

PALS is a unique and valuable technique which can characterize the free-volume hole properties in solid polymeric systems based on the detection of two γ -rays emitted from the birth and death of positrons. When positrons from a source are injected into a sample, they either (i) diffuse into the media and become annihilated as a free positron in about 0.4 ns or (ii) capture an electron from the sample and form a bound-state positronium (Ps) of two spin states, i.e. *para*-Ps (*p*-Ps) or *ortho*-Ps (*o*-Ps). The *p*-Ps, in which the spins of two particles are antiparallel, decays in about 0.15 ns via self-annihilation, while

the *o*-Ps of parallel spin state is shifted and localized in the free volume holes. The *o*-Ps has an intrinsic lifetime of 142 ns in a vacuum. However, in polymer, the *o*-Ps lifetime is shortened to a few nanoseconds through the interaction with the molecules constituting the wall of free volume hole. The *o*-Ps lifetime has been proven to be highly correlated with the average size (radius, R of $\sim \text{\AA}$) and distribution of hole space in the samples; the longer the lifetime of *o*-Ps, the larger the R , and vice versa [25,26]

$$\tau_{o\text{-Ps}} = \frac{1}{2} \left[1 - \frac{R}{R_0} + \frac{1}{2\pi} \sin\left(\frac{2\pi R}{R_0}\right) \right]^{-1} \quad (3)$$

where $\tau_{o\text{-Ps}}$ is annihilation lifetime of *o*-Ps (ns), R is size (radius) of free hole space (Å), and R_0 is $R + \Delta R$ where the fitted empirical electron layer thickness ΔR is 1.66 Å.

Fig. 10 shows the continuous positron lifetime distributions of PVC/HPCL–TiO₂ with UV illumination analyzed by the maximum entropy method using MELT program. It is worth to note that the first component with the shortest lifetime, τ_1 (~0.15 ns) is related to the annihilation of *p*-Ps, and the second component with the lifetime, τ_2 (0.3–0.4 ns) is due to the annihilation of positrons that does not form Ps, i.e. free positron. The last component with the longest τ_3 (1–5 ns) is the *o*-Ps lifetime which has an adequate correlation with the property of molecular-level free volume in samples. The lifetime distribution peaks exhibit three well-defined peaks and the widths of τ_3 indicative of the distributions of free volume size grow bigger with the increase of the UV irradiation, which may be attributed to polydispersity of the irradiated samples due to photocatalytic degradation, as was confirmed in the molecular weight distribution in Fig. 9.

In the finite term lifetime analysis through PATFIT program, the number of components is fixed with that of the MELT result. Fig. 11 shows the discrete average values of *o*-Ps lifetime and intensity against irradiation time. The measured *o*-Ps lifetime of PVC/HPCL–TiO₂ corresponds to the free volume space of radius from 2.84 to 2.95 Å. The decrease of *o*-Ps lifetime indicates that the UV irradiation causes the contraction of the molecular-sized free volumes, which is more distinguishable in the PVC/HPCL–TiO₂ than that of PVC/HPCL. The combined consideration with UV–visible and GPC results of Figs. 8 and 9 suggest that the size decrease might be attributed to the collapse of free volume due to chain scission or the formation of intramolecular double bonds and/or intermolecular crosslink through the recombination of PVC radicals.

The *o*-Ps intensity, I_3 can be a measure of the relative number concentration of free cavity sites in the samples and additionally the chemical environment caused by polar atoms and groups which can influence the trapping rate of *o*-Ps in the free volume to the considerable extent. For example, from the

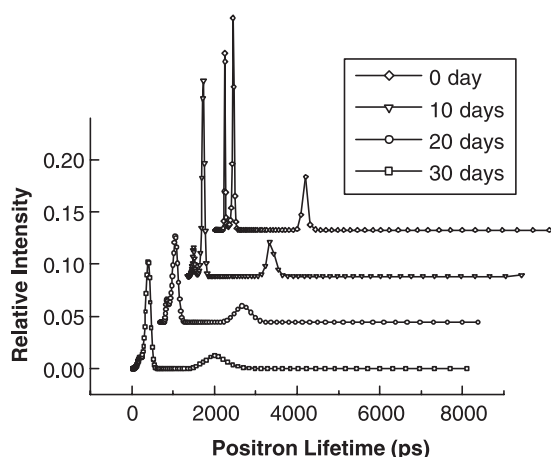


Fig. 10. Positron lifetime distribution of PVC/HPCL–TiO₂.

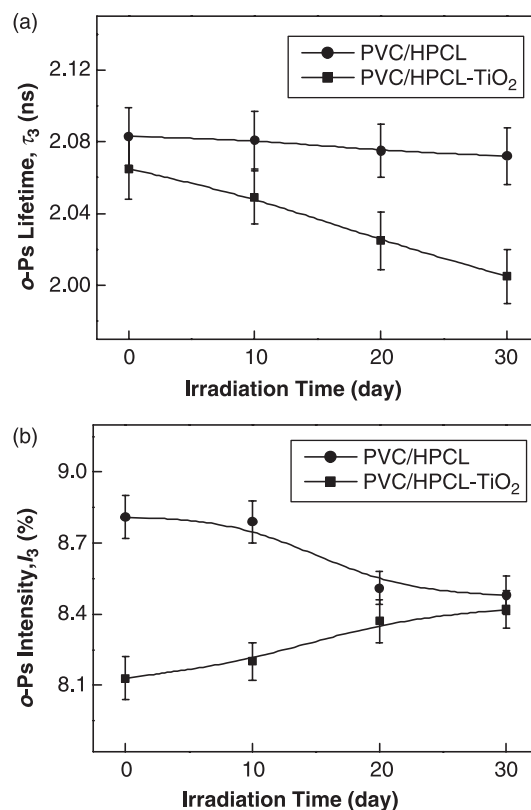


Fig. 11. *o*-Ps lifetime, (a), and intensity, (b), in both PVC/HPCL and PVC/HPCL–TiO₂ samples.

supporting results not shown in this paper, we saw that the *o*-Ps intensity was decreased with increasing the contents of conjugated double bond in PVC. The slight decrease of I_3 in the PVC/HPCL is due to the formation of conjugation bonds through photolytic degradation of PVC. In case of the PVC/HPCL–TiO₂, the UV illumination on samples causes the increase in the *o*-Ps intensity although a number of conjugated double bonds are also formed as shown in Fig. 11. This result shows that the increase in the number of chain ends accompanied by the successive chain cleavage predominates over the formation of conjugated double bonds in case of the PVC/HPCL–TiO₂ samples. The PALS results could show another complementary evidence of photocatalytic degradation of PVC/TiO₂ nanohybrid. Although the annihilation rate of positron in sample is affected on only a molecular-level free volume in radius of 0.5–10 Å, this study shows a possibility of PALS as a new tool to characterize the molecular level structural change and correlate it with macroscopic phenomena.

4. Conclusions

The poor dispersion of TiO₂ nanoparticles in PVC polymer has been known to be the main problem in the conventional PVC/TiO₂ composites. This study presented an innovative approach to prepare TiO₂ well-dispersed PVC/TiO₂

nanohybrid and characterized the photocatalytic degradation behavior of the nanohybrid.

- (1) The modified hyperbranched poly(ϵ -caprolactone) (HPCL) which has numerous $-\text{COOH}$ functional ends and good miscibility with PVC was used as a binder for the introduction of TiO_2 into PVC. The TiO_2 was first incorporated with the HPCL (HPCL) through the self-assembly process and then the HPCL– TiO_2 was blended with PVC without forming TiO_2 agglomerates.
- (2) The spectroscopic analysis demonstrated that TiO_2 nanoparticles were well dispersed in the PVC/HPCL– TiO_2 nanohybrid as compared with the conventional PVC/ TiO_2 with containing a similar content of TiO_2 .
- (3) The structural changes of PVC/ TiO_2 nanohybrid after the UV irradiation were analyzed by various characterization methods, such as FE–SEM, UV–visible spectroscopy, GPC, and PALS. These results showed the evidence for the photocatalytic degradation of the PVC/ TiO_2 nanohybrid and its potential for possible use as an eco-friendly alternative for the disposal of PVC wastes to the current waste landfill and dioxin-generating incineration.

Acknowledgements

The authors are grateful to the Ministry of Environment of Republic of Korea for their support under the grant for Eco-Technopia 21 project.

References

- [1] Mark HT, Bikales NM, Overberger CG, Menges G, Kroschwitz JJ. Encyclopedia of polymer science and engineering. New York: Wiley; 1985.
- [2] Hidaka H, Suzuki Y, Nohara K, Horikoshi S, Hisamatsu Y, Pelizzetti E, et al. *J Polym Sci* 1996;34:1311.
- [3] Horikoshi S, Serpone N, Hisamatsu Y, Hidaka H. *Environ Sci Technol* 1998;32:4010.
- [4] Cho S, Choi W. *J Photochem Photobiol, Part A: Chem* 2001;143:221.
- [5] Mills A, Hunte SL. *J Photochem Photobiol, Part A: Chem* 1997;108:1.
- [6] Zan L, Tian L, Liu Z, Peng Z. *Appl Catal, Part A: Gen* 2004;264:237.
- [7] Frechet JMJ. *Science* 1994;263:1710.
- [8] Trollsas M, Hedrick JL. *Macromolecules* 1998;31:4390.
- [9] Sivalingam G, Karthik R, Madras G. *Polym Degrad Stab* 2004;84:345.
- [10] Choi J, Kwak S-Y. *Macromolecules* 2003;36:8630.
- [11] Choi J, Kwak S-Y. *Macromolecules* 2004;37:3745.
- [12] Liu Y, Wang A, Claus R. *J Phys Chem, Part B* 1997;101:1385.
- [13] Shin H, Collins RJ, De Jguire MR, Heuer AH, Sukenik CN. *J Mater Res* 1995;10:692.
- [14] Kwak S-Y, Kim SH, Kim SS. *Environ Sci Technol* 2001;35:2388.
- [15] Kim T-H, Sohn B-H. *Appl Surf Sci* 2002;201:109.
- [16] Lee SJ, Han SW, Yoon M, Kim K. *Vib Spectrosc* 2000;24:265.
- [17] Choi W, Termin A, Hoffmann MR. *J Phys Chem* 1994;98:13669.
- [18] Corey EJ, Schmit G. *Tetrahedron Lett* 1979;399.
- [19] Kirkegaard P, Eldrup M, Mogensen OE, Pedersen N. *Comput Phys Commun* 1981;23:307.
- [20] Shukla A, Peter M, Hoffmann L. *Nucl Instrum Methods, A* 1993;335:310.
- [21] Flory PJ. *J Am Chem Soc* 1952;75:2718.
- [22] Torikai A, Hasegawa H. *Polym Degrad Stab* 1999;63:441.
- [23] Owen ED. *Degradation and stabilization of PVC*. London: Elsevier; 1984.
- [24] Suvegh K, Klapper M, Domjan A, Mullins S, Wunderlich W, Vertes A. *Macromolecules* 1999;32:1147.
- [25] Tao SJ. *J Phys Chem* 1972;56:5499.
- [26] Nakanishi H, Jean YC. In: Schrader DM, Jean YC, editors. *Positron and positronium chemistry*. Amsterdam: Elsevier Science; 1988. p. 159–92.